Theoretical Analysis and Design of a Double-Clamped Microchannel Resonator

by

Joshwa Wang

SUBMITTED TO THE DEPARTMENT OF MECHANICAL ENGINEERING IN PARTIAL FULFILLMENT OF THE REQUIREMENTS FOR THE DEGREE OF

BACHELOR OF SCIENCE
AT THE
MASSACHUSETTS INSTITUTE OF TECHNOLOGY

JUNE 2007

Signature of Author: _____

Department of Mechanical Engineering
11 May 2007

Certified by: _____

Scott R. Manalis
Associate Professor of Biological and Mechanical Engineering
Thesis Supervisor

Accepted by: _____

John H. Lienhard V
Professor of Mechanical Engineering
Chairman, Undergraduate Thesis Committee

Theoretical Analysis and Design of a Double-Clamped Microchannel Resonator

by

Joshwa Wang

Submitted to the Department of Mechanical Engineering
on May 11, 2007, in Partial Fulfillment of the
requirements for the Degree of Bachelor of Science in
Mechanical Engineering.

ABSTRACT

The Suspended Microchannel Resonator (SMR) that is currently being used by the Nanoscale Sensing Group is the inspiration for this thesis. This work examines Master's degree candidate Sungmin Son's theoretical analysis of a cantilevered microchannel beam that is fixed at both ends. The current design used in lab is a traditional cantilevered beam and has been successful in producing results in the detection of biological molecules. This new design is an experiment on whether adequate mass sensitivity, readability, and reliable range can be reproduced using a different type of boundary condition and alternate geometry. My thesis will analyze Son's work to determine what types of mass sensitivity, readability, and reliable range can be achieved by altering the microchannel geometry.

Thesis Supervisor: Scott R. Manalis
Title: Associate Professor of Biological and Mechanical Engineering

Table of Contents

1. Introduction....4
1.1 Purpose....4
1.2 Project Overview....4
1.3 Organization....4
1.4 Acknowledgements....5
2. Project Background....5
2.1 Quartz-Crystal Microbalance....5
2.2 Surface Plasmon Resonance....5
2.3 Suspended Microchannel Resonator....5
3. Double-Clamped Microchannel Resonator....6
3.1 Theoretical Analysis....6
3.1.1 Equation of Motion....6
3.1.2 Boundary Conditions....7
3.1.3 Solution for Resonant Frequency of Overpass....7
3.2 Mass Sensitivity....9
3.3 Readability....9
3.4 Reliable Range....10
4. Alternate Designs....13
5. Results....14
5.1 Mass Sensitivity Analysis....14
5.2 Readability....14
5.3 Reliable Range....16
6. Design Issues....18
6.1 Fatigue Failure....18
6.2 Particle Deviation....19
7. Conclusions....20

1. Introduction

Currently in the field of biomedical devices there is a need for real-time, high throughput detection of molecular interactions. The Nanoscale Sensing Group has utilized a device known as the Suspended Microchannel Resonator (SMR) designed by Thomas Burg of the group to detect interactions such as binding between avidin and biotinylated serum albumin. The SMR relies on detecting shifts in resonant frequency of the cantilevered, suspended microfluidic channel as biological molecules accumulate within the channel. Sungmin Son of the Nanoscale Sensing Group has analyzed the feasibility as well as the unique characteristics that can observed by using a microfluidic channel that is anchored from both ends as opposed to being cantilevered. By varying the geometry of the microfluidic or "overpass" channel, the mass sensitivity, readability, and reliable range may be manipulated to produce results that are adequate for use in experiments.

1.1 Purpose

We would like to analyze the feasibility of using alternate geometries and boundary conditions for a double-clamped overpass channel. From these analyses we should gain a greater understanding of whether this is possible while still maintaining adequate mass sensitivity, readability, and reliable range for the detection of biological molecules and their interactions.

1.2 Project Overview

This project stemmed from the device that is currently being used by the Nanoscale Sensing Group here at MIT. They currently use a cantilevered microfluidic channel more commonly known as the Suspended Microchannel Resonator (SMR). Using this device one can measure the mass of biological molecules by monitoring the change in resonant frequency of the beam as a particle is passed within it. Sungmin Son of the group began experimenting with the idea of implementing a double-clamped beam and altering the geometry to observe what the feasibility was of exploring other geometries.

1.3 Organization

This report will give an overview and analysis of the design of a double-clamped microchannel resonator. Section 2 will provide background information and the current methods being employed in biological detection. Section 3 will give a theoretical analysis for the double-clamped microchannel resonator that Son worked on. Section 4 covers alternate designs for a double-clamped overpass channel and a comparison of their attributes. Section 5 will cover the results from Matlab and Ansys analysis of the double-clamped channel and the alternate designs. Section 6 considers design issues that are important in the design of the double-clamped microresonator. Finally section 7 will conclude this thesis and offer suggestions for future research.

1.4 Acknowledgements

I would like to thank Professor Scott Manalis and everyone at the Nanoscale Sensing Group at MIT. It was a good experience getting to know everyone in the lab and learning from their experience. In particular I would like to extend my deepest gratitude to Sungmin Son who began to explore the idea behind my thesis. Without all these individuals this thesis would never have come to fruition.

2. Project Background

The desire to understand and detect biological molecules with high accuracy and high-throughput has led to the advent of various devices used to aid researchers. Each device has advantages and disadvantages depending on the matter being detected and how much resolution, accuracy, and precision are needed in the measurements. These devices fall into a broad category known as biosensors. Generally, the sensor is attached to a processing unit which converts a response (the binding of biological molecules or the presence of a cell) into a change in electrical or optical signal. This output provides useful information that may be analyzed. The SMR falls into a specific class known as label-free biosensors. That is, the sample molecules do not require preparation or fluorescent labeling which can interfere with the biological interactions that one may wish to study. Currently, prominent label-free biosensing techniques are the quartz-crystal microbalance (QCM) and surface plasmon resonance (SPR).

2.1 Quartz Crystal Microbalance

The QCM utilizes and piezoelectric quartz crystal which changes in resonant frequency when disturbed by an external mass upon its surface. By determining the change in resonant frequency of the quartz crystal, one may calculate the mass of the particle on the surface or determine the thickness of a film deposited upon it. Although this method provides mass resolution in the nanogram range, it requires a large sample volume (10-1000 μL) and is less sensitive than fluorescence screening.

2.2 Surface Plasmon Resnonance

SPR is another type of label-free detector that uses optical detection techniques. This method may be used to characterize the interactions of various biopolymers, including protein-ligand, protein-protein, protein-DNA, and protein-membrane binding. Specifically, SPR can also be used to quantify the equilibrium constants and kinetic constants. The major drawbacks on using SPR are the large and expensive instrumentation as well as the large sample volumes (greater than 100 μL) needed.

2.3 Suspended Microchannel Resonator

The device currently used by the Nanoscale Sensing Group counters many of the downsides found in its label-free counterparts. Rather than requiring large sample volumes like QCM or SPR, the SMR can work even with only picoliter sample volumes. Detection with the SMR requires determining the shift in resonant frequency of a suspended microfluidic channel as

molecules gather along the inner wall. The SMR is actuated using electrostatic force and can be interfaced directly with conventional microfluidic systems.

3. The Double Clamped Microchannel Resonator

For the theoretical design of the double-clamped microchannel resonator, there are three matters of concern. First, the device must have at least a mass resolution of 10^{-17} g/μm^2 (the current mass resolution of the SMR). Second, the amplitude of oscillation for the microchannel must be large enough to be detected using the optical setup used for the SMR. Finally, the reliable range must be long enough so that an adequate measurement may be made as a biopolymer travels along the length of the microfluidic channel.

To this end, Sungmin Son has explored the possibility and has conducted a theoretical analysis of the feasibility of such an idea. To conclude, he has considered some other issues that would need to be taken into account for the double-clamed microchannel resonator to come to fruition. The issues being fatigue failure (how many oscillation the microchannel may sustain) and particle deviation which may cause variance in output frequency due to the position of the particle along the lateral width of the beam.

3.1 Theoretical Analysis

As mentioned previously the primary objectives are to achieve high mass sensitivity, large oscillation amplitude, and long reliable range. To proceed with the analysis it is helpful to understand some assumptions that are made at the beginning. First, gravitational effects are ignorable as mentioned in the MEMS source book. Second, pressure effect within the microfluidic channels is negligible as discussed in Thomas Burg's doctoral thesis. Finally, axial force as the microchannel is oscillating is negligible. This was verified analytically using Ansys FEA software package.

3.1.1 Equation of Motion

The following figure shows a basic drawing of the double-clamped beam oscillating in its first mode shape.

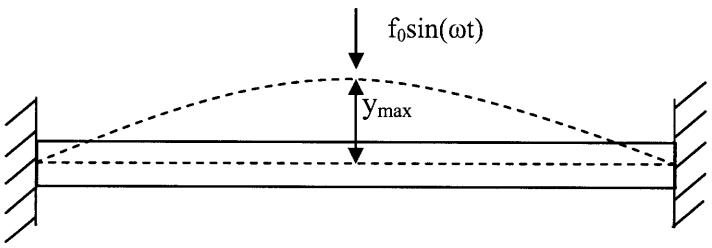

Figure 1. This figure shows the maximum oscillation of the double clamped beam in its first mode shape and the sinusoidal electrostatic force imparted onto the beam.

In the figure f_0 is the electrostatic force applied to the double-cantilevered beam and y_{max} is the maximum displacement at the center of the beam.

Generally the equation of motion for a beam with respect to distance from the origin and time is

$$f(x,t) = \rho A \frac{\partial^2 y}{\partial t^2} + EI \frac{\partial^4 y}{\partial x^4} + c \frac{\partial y}{\partial t} \tag{1}$$

where ρ is the density, A is the cross-sectional , E is the Young's Modulus, I is the area moment of inertia of the beam. The damping constant is c.

3.1.2 Boundary Conditions

The double-clamped beam has the following boundary conditions

$$y(x,t)\Big|_{x=0} = 0 \tag{2}$$

$$\left.\frac{\partial y(x,t)}{\partial x}\right|_{x=0} = 0 \tag{3}$$

$$y(x,t)\Big|_{x=L} = 0 \tag{4}$$

$$\left.\frac{\partial y(x,t)}{\partial x}\right|_{x=L} = 0 \tag{5}$$

Equations 2 and 4 describe the fixed nature of the two ends of the beam while equations 3 and 5 indicate that the velocity at the ends of the beams will remain at zero for all time. These boundary conditions are necessary for solving the equation of motion for the beam.

3.1.3 Solution for Resonant Frequency of Overpass

To solve for the resonant frequency in the first mode shape of the double-clamped beam separation of variables must be used. To solve equation 1 use the following general equation

$$y(x,t) = a(x)e^{\omega t} \tag{6}$$

Substituting equation 6 back into equation 1 the following equation is derived

$$\rho A \omega^2 a + EI \frac{d^4 a}{dx^4} + c\omega a = 0 \tag{7}$$

where ω is the frequency of oscillation. Separation of variables requires that

$$\frac{d^4 a}{dx^4} = \lambda^4 a \tag{8}$$

and solving equation 7 for λ gives

$$\lambda^4 = -\frac{\rho A \omega^2 + c\omega}{EI} \tag{9}$$

From the boundary conditions of the overpass at either fixed end

$$a(x = 0, L) = \frac{da}{dx} = 0 \tag{10}$$

where L is the length of the double-clamped microchannel. The general equation for a vibrating system

$$a_1(x) = c_1(-0.9825 \sin \lambda x + \cos \lambda x + 0.9825 \sinh \lambda x - \cosh \lambda x) \tag{11}$$

along with the boundary conditions given in equation 10 yields a constant

$$(\lambda L)_1 = 4.73 \tag{12}$$

for the first mode shape of vibration.

Using the quadratic method to solve equation 9, the frequency of the overpass channel is derived

$$\omega = \frac{-c \pm \sqrt{c^2 - 4EI\rho A\lambda^4}}{2\rho A} \tag{13}$$

To determine the resonant frequency of the beam, the imaginary portion of the quadratic solution in equation 13 is used

$$\omega_r = \frac{\sqrt{4EI\rho A\lambda^4 - c^2}}{2\rho A} \tag{14}$$

For purposes of this theoretical analysis the damping coefficient is considered sufficiently low such that c is approximately zero. Therefore

$$\omega_r = \omega_{r0}\sqrt{1 - \varsigma^2} \tag{15}$$

Where ζ=3.33X10^{-5} when the quality factor is Q=15,000. This value for the quality factor comes from Thomas Burg's thesis and is a benchmark value used for the suspended microchannel resonator in vacuum. Since the damping ratio is very low

$$\omega_r \cong \omega_{r0} \tag{16}$$

Using the relationship given in equation 15 and the assumptions made for ζ, the equation for the resonant frequency is given by

(17) $$\omega_{r0} = \lambda^2 \sqrt{\frac{EI}{\rho A}}$$

3.2 Mass Sensitivity

To determine the mass sensitivity of the double-clamped overpass channel, the mode shape as well as the relationship between the frequency and the mass of the particle traveling within the channel must be considered. For each mode shape

(18) $$\lambda L = C$$

where C is a constant dependant on the mode shape of vibration. In the first mode shape C equals 4.731. The following is the general equation of the resonant frequency for a beam with respect to mass and volume

(19) $$\omega = C^2 \sqrt{\frac{EI}{mL^3}}$$

The derivative of the frequency with respect to mass is

(20) $$\frac{d\omega}{dm} = -\frac{1}{2}\frac{C^2\sqrt{EI}}{L^{3/2}} m^{-3/2}$$

By dividing equation 20 by equation 19, the relationship between mass and the change in frequency is found to be inversely proportional to mass or

(21) $$\frac{d\omega/dm}{\omega} = -\frac{1}{2m}$$

Therefore, the sensitivity is mainly dependent o the mass of the beam.

3.3 Readability

The readability of the signal from the overpass channel pertains to the amplitude with which it oscillates. The channel must have a large enough amplitude such that the detection device can notice a change in its position and thereby be able to turn it into a signal which may be processed. In our theoretical analysis of the readability of the overpass channel, two main assumptions are made. First, the thermal noise will be ignored. Second, it is assumed that the forcing function has exactly one frequency. From equation 1 presented earlier we may further specify the force along the length of the overpass channel with the following function

(22) $$\rho A \frac{\partial^2 y}{\partial t^2} + EI \frac{\partial^4 y}{\partial x^4} + c\frac{\partial y}{\partial t} = f_0 \delta\left(x - \frac{L}{2}\right)\sin \omega t$$

The delta function denotes the fact that force is applied nowhere along the length of the beam except directly along the lateral centerline. Since there are infinitely many modes of vibration, it is necessary to define the possible combinations of vibration defined here by the summation of the general form of various mode shapes

$$y(x,t)=\sum_{j=1}^{\infty} a_j(x)u_j(t) \tag{23}$$

Placing equation 23 into equation 22 gives

$$\sum \rho A\frac{\partial^2 u_j}{\partial t}a_j+\sum EI\frac{\partial^4 a_j}{\partial x^4}u_j+\sum c\frac{\partial u_j}{\partial t}a_j=f_0\delta\left(x-\frac{L}{2}\right)\sin\omega t \tag{24}$$

By the principle of orthogonality, this equation becomes

$$\frac{\partial^2 u}{\partial t^2}+\frac{c}{\rho A}\frac{\partial u}{\partial t}+\frac{EI}{\rho A}\lambda^4 u=\frac{1.58816}{4.73017\rho A}\frac{f_0\lambda}{C_1}\sin\omega t \tag{25}$$

To find the magnitude of oscillation for the first mode shape, the absolute magnitude of the displacement equation is taken at the center of the double-clamped overpass channel.

$$\left|y_1(x,t)\right|=\left|a_1\left(\frac{L}{2}\right)u_1(t)\right|=\frac{0.5332f_0\lambda}{\rho A}\frac{1}{\sqrt{\left(\frac{c\omega}{\rho A}\right)^2+\left(\omega_{r0}{}^2-\omega^2\right)^2}} \tag{26}$$

When, $\omega=\omega_{r0}$

$$\left|y_1(x,t)\right|=\frac{0.5332L^2\lambda}{4.73^2 c}\sqrt{\frac{\rho A}{EI}}=\frac{2.51929\times10^{-3}L^3}{EI\zeta} \tag{27}$$

To compare with the current, cantilevered design the boundary conditions can be adjusted to find that

$$\left|y_1(x,t)\right|=\frac{4L^2\lambda}{1.87978c3.52}\sqrt{\frac{\rho A}{EI}}=\frac{0.161166L^3}{EI\zeta} \tag{28}$$

3.4 Reliable Range

The reliable range refers to the distance along the length of the overpass channel where the frequency of the overpass channel is accurate enough to be used for data collection. When measuring a particle or point mass using the overpass channel, the frequency will fluctuate until the particle arrives at the center where there is maximum frequency shift. Their should be a length of channel on either side of this center point for which the frequency shift is close enough to the maximum such that the frequency shift measurement may still be used. Son defines this variable as

(29) $$R_{rel} = \frac{t_{rel}}{t_{total}}$$

where t_{rel} is the total length of the reliable range, t_{total} is the length of the beam, and R_{rel} is the ratio of the two lengths.

The following illustration visually represents the idea presented above

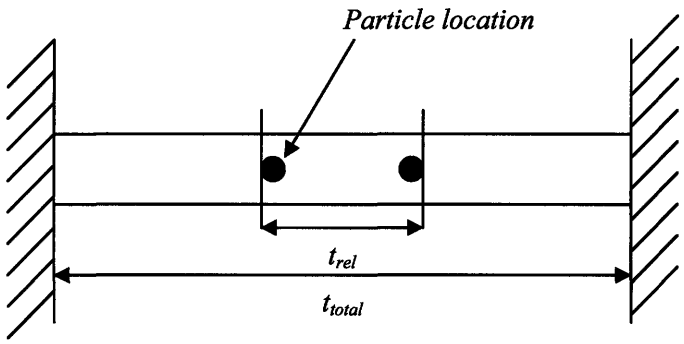

Figure 2: This diagram defines the reliable range of the overpass channel. This is of importance because the usefulness of the device depends on how much time useful data may be collected from the overpass channel device.

To determine the reliable range, the variance in frequency as a particle of specified mass travels along the channel was calculated. The admissible variance in this case was defined as 5% above or below the resonant frequency when the particle is exactly in the middle of the overpass channel. The following figure defines some variable necessary to theoretically calculate the admissible variance

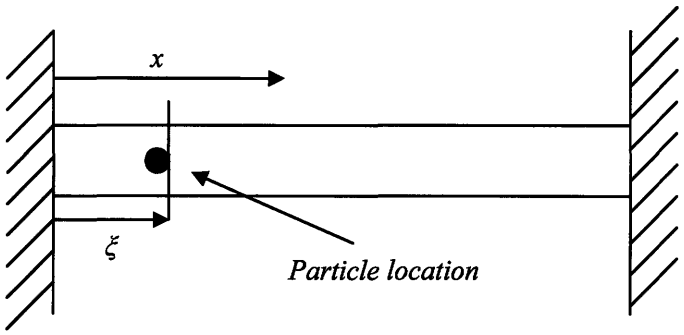

Figure 3: This drawing defines variable necessary to determine the reliable range of the overpass channel with a 5% admissible variance in output frequency.

Using the Lagrangian equation, equation 12 may be recalculated to determine the frequency as a function of particle distance from the entry point of the overpass channel. The Lagrangian equation with respect to the particle distance is

(30) $$y = \sum \phi_j X_j$$

The admissible variance is defined as

(31) $$\delta y = \delta\phi_1 X_1$$

Here, X_1 is defined as

(32) $$X_1 = C_1(-0.9825\sin\lambda x + \cos\lambda x + 0.9825\sinh\lambda x - \cosh\lambda x)$$

Determining the reliable range of the overpass channel requires consideration of the work done by inertial force and the work done by elastic force. The work done by the inertial force is defined as the following

(33) $$-\rho A\int_0^L \ddot{y}\delta y dx$$

Substituting the equation 31 and the second derivative of equation 30 into equation 33

(34) $$-\rho A\ddot{\phi}_1\delta\phi_1\int_0^L X_1^{\,2}dx$$

Integrating gives

(35) $$-\rho A\ddot{\phi}_1\delta\phi_1\frac{4.7307}{\lambda}C_1^{\,2}$$

Finally replacing the density and area terms, the inertial contribution is defined as

(36) $$\Delta m\ddot{\phi}_1 X_1(\zeta)\delta y = \Delta m\ddot{\phi}_1 X_1(\zeta)^2\delta\phi_1$$

where ζ indicates the position along the overpass channel and m is the mass of the channel. The elastic force contribution is defined as

(37) $$EI\phi_1\lambda^4\frac{4.73017}{\lambda}\delta\phi_1 C_1^{\,2}$$

Summing up the contributions from the inertial and elastic components, another form of the equation of motion is derived

(38) $$\left(\rho A\frac{4.73017}{\lambda} + \Delta m X_1^{\,2}\right)\ddot{\phi}_1 + 4.73017EI\lambda^3\phi_1 = 0$$

Therefore, the frequency is

(39)
$$\omega = \sqrt{\frac{4.73017EI\lambda^3}{\frac{4.73017\rho A}{\lambda} + \Delta m X(\zeta)^2}}$$

4. Alternate Designs

Son originally analyzed three different variations on the double-clamped overpass channel. The first was a channel with normal dimensions comparable to that of the suspended microchannel resonator width. The second was an overpass channel that tapered in from the center and decreased in channel width as it approached either end point. Finally, a third design with narrow channel width was analyzed. The following dimensioned drawings provide a clearer explanation of the geometry.

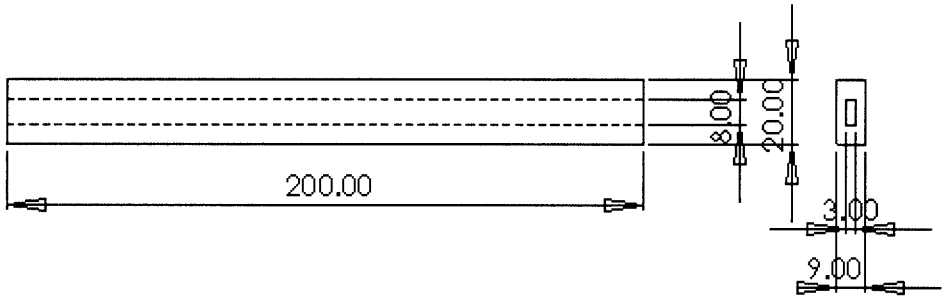

Figure 4: This drawing shows the dimensions for the original overpass design. All units are in micrometers.

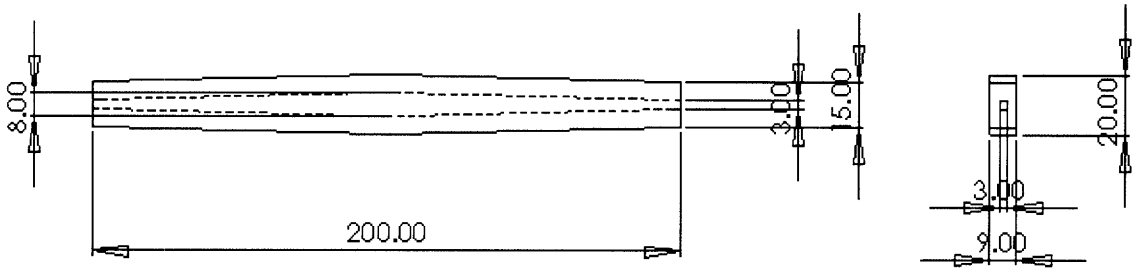

Figure 5: This drawing shows dimensions for the tapered overpass channel. The ratio of the widest to narrowest cross-section width is 4:3.

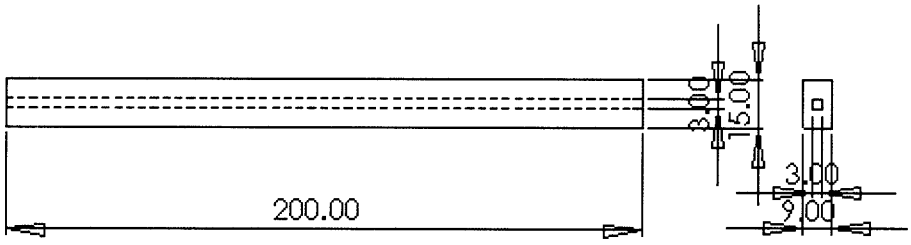

Figure 6: This drawing shows dimensions for the narrow overpass channel. The cross-sectional width of this channel is equivalent to the narrowest dimension of the tapered overpass channel.

Normalizing the three main factors of importance in the alternate designs, mass sensitivity, readability, and reliable range, with that of the original overpass channel yielded the following results

	Mass sensitivity	Readability	Reliable range
Straight	1	1	1
Tapered	1.14	1.23	1.57
Narrow Straight	1.33	1.33	1

Table 1: This table compares the attributes of the 3 designs discussed above.

5. Results

The response of the overpass channel was determined through both analysis using Matlab as well as finite element analysis using Ansys. The results of determining the mass sensitivity, readability, and reliable range of the overpass channel are presented here as well as a comparison of the current method which employs the use of a suspended microchannel resonator.

5.1 Mass Sensitivity Analysis

As proven analytically, the mass sensitivity is inversely proportional to the mass of the beam. Therefore as the beam increases in mass the sensitivity or resolution of the output frequency shift will decrease. Adequate mass sensitivity is considered to be 10^{-17} grams per micrometer. The current design of the double-clamped channel verified that the mass sensitivity is adequate for making measurements involving biological molecules.

5.2 Readability

Comparison of readability or oscillation amplitude was made analytically between the single-clamped cantilevered channel and the double-clamped overpass channel. The resonant frequencies were determined using Matlab and Ansys analysis. The following plot shows the resonant frequency peaks and amplitude of oscillation.

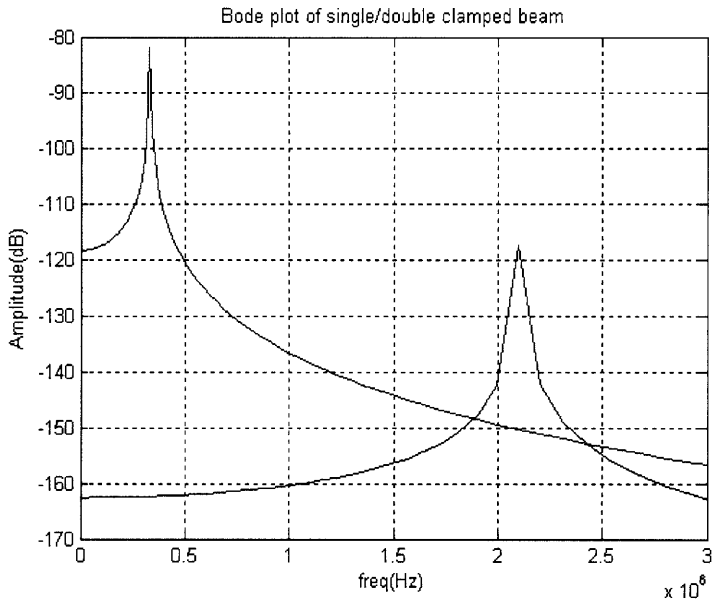

Graph 1: Using Matlab analysis the above plots were made. The blue curve is the bode plot of the single-clamped beam currently being used which had a resonant frequency of 330.73 kHz. The red curve is the bode plot of the theoretical overpass channel which has a resonant frequency of 2102.1 kHz.

The following table compares the single clamped cantilever with the overpass channel designed by Son. Matlab and Ansys were used to determine the resonant frequency of the two microfluidic channels.

	Resonant Frequency (kHz)		Magnitude	
	Matlab	Ansys	Matlab	Ansys
Cantilever	330.73	330.22	0.16772μm	0.168371μm
Overpass	2102.1	2100(2D) 2198(3D)	2.6218nm	2.62227nm(2D) 2.41132nm(3D)

Table 2: The data serves as a comparison and shows agreement between the theoretical and finite element analyses.

Analysis has shown that readability is much higher for the single-clamped cantilever. The cantilever had an amplitude approximately 64 times larger than that of the overpass. In order to achieve the similar oscillation amplitudes for the overpass, it must be longer by four times the current size. The following equation can be used to address these major issues and guide future designs.

(40) $$|y_1(x,t)| = \frac{2.51929\times10^{-3}L^3}{EI\zeta}$$

In order to increase the amplitude while still maintaining equivalent mass sensitivity, the wall thickness could be changed to increase the stiffness or the profile of the overpass may be altered.

5.3 Reliable Range

The theoretical analysis yielded the following results. Two particles, one weighing 1 picogram, the other weighing 1 nanogram were used to benchmark reliable ranges to within a 5% admissible variation for frequency shift. The reliable range for the picogram-sized particle was 22 micrometers while the reliable range for the nanogram-sized particle was 62 micrometers.

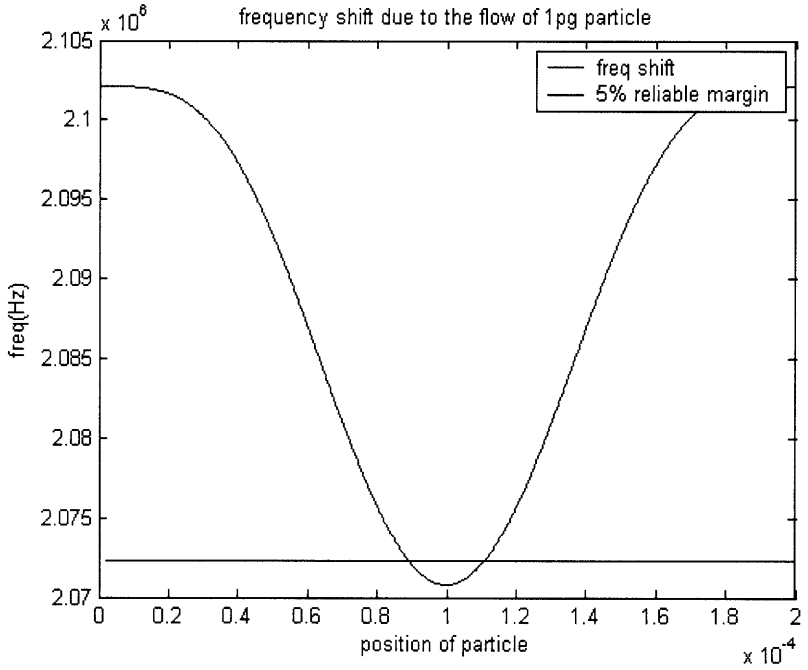

Graph 2: The graph above plots the 5% admissible variation for frequency and the frequency shift as a one pictogram particle travels along the length of the over pass channel.

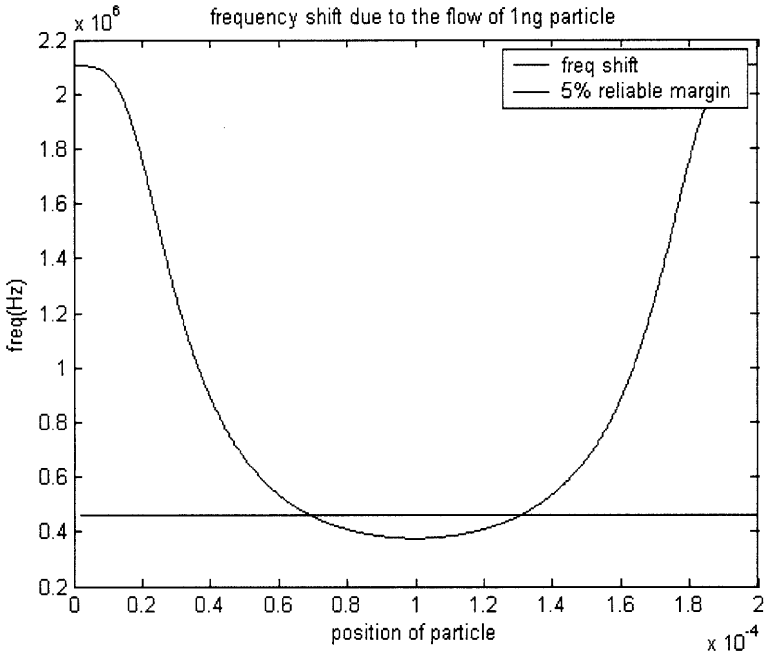

Graph 3: The graph above plots the 5% admissible variation for the frequency and the frequency shift as the nanogram-sized particle travels the length of the overpass channel.

A comparison was made between the analytical solutions produced by Matlab and the Ansys results when a 1 nanogram particle flowed through the overpass.

(41)
$$D_{rel} = \frac{F_{margin} - F_{center}}{F_o - F_{center}} \times 100(\%)$$

In equation 41 F_{margin} is the 5% variation of the resonant frequency when the particle is at the center of the overpass, F_{center} is the resonant frequency when the particle is at the center of the overpass, F_0 is the resonant frequency of the overpass, and D_{rel} is the reliable distance of the overpass. The following table outlines the findings

	Matlab	3D straight	3D tapered
F_0(Hz)	0.21×10^7	0.21×10^7	0.20×10^7
F_{center}(Hz)	3.75×10^5	0.77×10^6	0.64×10^6
F_{margin}(Hz)	4.61×10^5	0.84×10^6	0.71×10^6
D_{rel}(μm)	62	44.4	63.4
R_{rel}(%)	31	22.2	34.8

Table 3: The table above compares the results from the Matlab results and the 3D Ansys results. The 3D narrow design was not considered during this analysis.

6. Design Issues

Son originally considered a couple of design problems that are of importance in the design of an overpass channel. The first is the possibility of fatigue failure. Fatigue failure is caused by the high cycle life that the overpass channel must withstand. It is important to keep this in mind as a decrease in the integrity of the channel may lead to inaccurate frequency shift measurements and subsequently inaccurate mass measurements. The second concern does not deal with the structure of the overpass channel but with the accuracy of placing a particle. Son has defined this issue as particle deviation. Particle deviation may cause inaccuracies in the frequency measured due to the lateral location along the width of the overpass channel where the particle resides during its travel along the length of the channel.

6.1 Fatigue Failure

Fatigue failure can arise from the displacement that the overpass channel experiences as it is placed under electrostatic force. Given fatigue stress, Y_{max} is proportional to length L, the length of the overpass channel

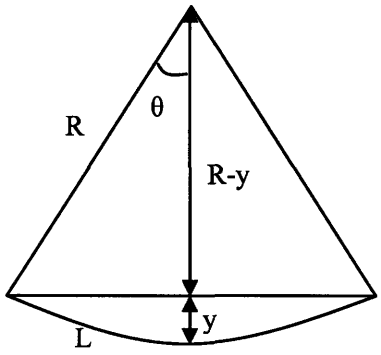

(42) $$L = 2R\theta$$

Basic geometry identities indicate

(43) $$\theta = \cos^{-1}\frac{R-y}{R}$$

Substituting θ with equation 42

(44) $$\cos\frac{L}{2R} = \frac{R-y}{R}$$

In this case, since the overpass channel length is significantly less than its radius of curvature or $L<<R$ then

(45) $$\cos\frac{L}{2R} \cong \frac{L}{2R}$$

Therefore replacing the cosine function in equation 44 gives

(46) $$R = y + \frac{L}{2}$$

The magnitude of the fatigue stress of the overpass channel is calculated in the following manner

(47) $$\left|\sigma_{fat}\right| = \left|-\frac{M_z y_{\max}}{I}\right|$$

By definition $M_z = \frac{EI}{R}$ and substituting equation 46 into equation 49

(48) $$\left|\sigma_{fat}\right| = \left|-\frac{E}{y+\frac{L}{2}} y\right|$$

With some algebraic manipulation we find that

(49) $$y = \frac{L\sigma_{fat}/2}{E-\sigma_{fat}} \propto L$$

This equation shows that the displacement experienced by the overpass channel is proportional to the length of the overpass channel. Assuming that the fatigue stress is 2GPa under 10^7 cycles, we determine the relationship between the displacement and channel length to be defined as

(50) $$y = \frac{L\times 10^9}{190\times 10^9 - 2\times 10^9} = \frac{L}{188}$$

The following graph plots the fatigue failure limit for a given length as well as the magnitude of oscillation experienced as a function of the overpass length.

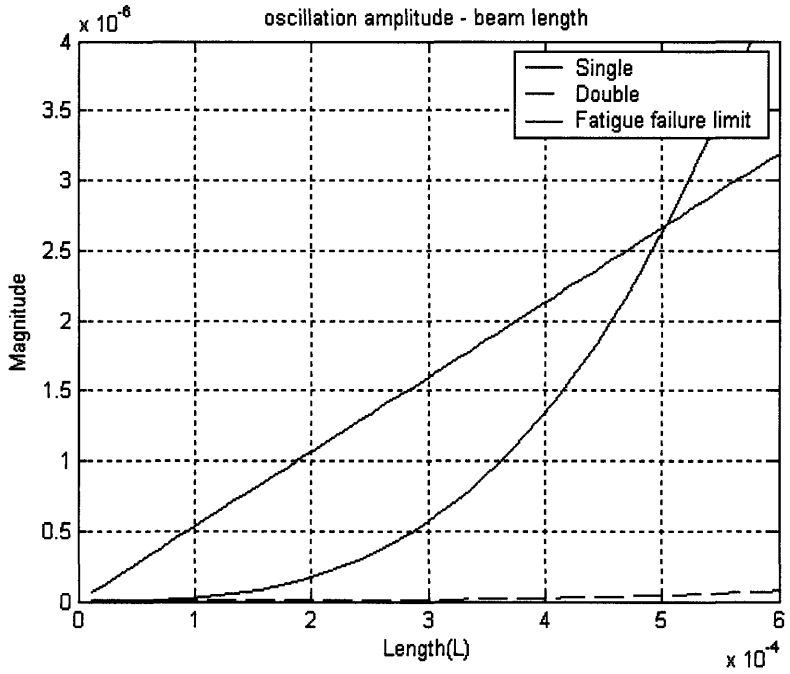

Graph 4: The plot above compares the oscillation amplitude of both the single-clamped and double-clamped microchannels with the absolute fatigue failure limit.

6.2 Particle Deviation

To determine whether the location of the particle laterally along the width of the channel was important or not, the resonant frequency was calculated for a point in both the center of the channel and the edge. Analysis shows that the change in frequency from when the point is at the center or the edge is not significant with only at most a .07% change in resonant frequency. The results are as follows

	Straight (Hz)	Tapered (Hz)
Center	0.77225×10^6	0.63803×10^6
Edge	0.77280×10^6	0.63825×10^6

Table 4: This table compares the resonant frequency of the original overpass channel and the tapered channel when the particle is at the center and when it is at the edge of the channel.

7. Conclusions

The double-clamped overpass channel has potential in becoming a useful alternative to the SMR. Sungmin's research provides parameters from which the overpass channel attributes may be specified. Mass sensitivity, readability, and reliable range can be altered by changing the geometry of the double-clamped overpass such that it produces comparable results currently

available. In the design of the overpass channel the mass must be minimized to obtain the highest frequency resolution. The length of the beam must also be optimized to provide high readability (oscillation amplitude). To prevent fatigue failure the amplitude of oscillation can be designed to be below the fatigue failure limit for the material.

Of the designs considered here, the two proposed by Son are the most feasible. The tapered design improves the reliable range while decreasing the mass sensitivity and readability. The narrow design has high mass sensitivity and readability but does not have improved reliable range. After considering the various designs, the tapered design proves to be the most advantageous one. Other designs would only be novel in nature and not help improve the sensitivity, readability, and range of the device.